

Photoinduced Redox Processes in Phthalocyanine Derivatives by Resonance Raman Spectroscopy

H. Abramczyk,* I. Szymczyk, G. Waliszewska, and A. Lebioda

Technical University, Department of Chemistry, Laboratory of Laser Molecular Spectroscopy at IARC 93-590 Łódź, Wróblewskiego 15, Poland

Received: September 6, 2002; In Final Form: September 30, 2003

Photochemical and photophysical behavior of copper(II) phthalocyanine-3,4',4'',4'''-tetrasulfonate anion $\text{Cu}(\text{tsPc})^{4-}$ irradiated with the visible light from the range 465–514 nm (vis) has been studied by resonance Raman spectroscopy. The photochemistry of monomers and dimers of $\text{Cu}(\text{tsPc})^{4-}$ has been studied in liquid solutions of H_2O and dimethyl sulfoxide (DMSO) as well as in crystal and glassy frozen matrixes as a function of temperature in the range 293–77 K. We have identified the transient species of the photoredox dissociation as ligand radicals $\text{Cu}^{\text{II}}(\text{tsPc}^\bullet)^{3-}$ and $\text{Cu}^{\text{II}}(\text{tsPc}^\bullet)^{5-}$. We have shown that the photoinduced dissociation with the electron transfer between the molecules of phthalocyanine is determined mainly by the molecular structure. The electron transfer that leads to the generation of the ligand-centered radicals may occur only for the ring-stacked structures with strong overlapping between the π -electronic clouds of the macrocycle rings of the adjacent molecules. These structures exist in highly concentrated aqueous solutions and in the crystal phases. The photoinduced electron transfer does not occur for the monomers of $\text{Cu}(\text{tsPc})^{4-}$ in DMSO solution and in the glassy phases. We have assigned the emission at 527 nm for $\text{Cu}(\text{tsPc})^{4-}$ in DMSO and at 556 nm in H_2O to the $T_n \rightarrow T_1$ fluorescence. Competitively, the higher excited triplet state T_n state (or the first excited singlet state S_1) participates in photoinduced redox dissociation $\text{Cu}(\text{tsPc})^{4-} \xrightarrow{h\nu} \text{Cu}^{\text{II}}(\text{tsPc}^\bullet)^{3-} + \text{Cu}^{\text{II}}(\text{tsPc}^\bullet)^{5-}$. The vis irradiation of the $\text{Cu}^{\text{II}}(\text{tsPc}^\bullet)^{3-}$ and $\text{Cu}^{\text{II}}(\text{tsPc}^\bullet)^{5-}$ radicals excites them to the lowest lying excited states that emit fluorescence at 682 nm after undergoing to the ground states.

1. Introduction

Phthalocyanines have well-established applications as green/blue pigments and as dyes. Their semiconducting properties have lead to significant efforts toward their incorporation in chemical sensors, their optoelectronic properties have profound influence on the progress in the materials area. Some phthalocyanines have been developed as photosensitizers in photodynamic therapy of cancer (PDT). Photodynamic therapy is a promising application of photodynamic activity. The literature has recorded reports related to photodynamic activity of phthalocyanines.^{1,2} They may overcome the major drawbacks of the porphyrine-type materials: skin photosensitivity, low selectivity for tumor tissue, long period of clearance from the body. It was found that both the central atom, the solvent, and the ligand substituents in phthalocyanines exert considerable influence on the sensitization activity. It was suggested that the activity decreases in the order $\text{Zn} > \text{Mg} > \text{Cu} > \text{Co} > \text{Fe}$.³ The zinc and aluminum complexes of sulfonated phthalocyanines have been developed as PDT agents in clinical use.⁴

A number of metallophthalocyanines exhibits a pronounced tendency to form polymers^{5–7}—polymer sheet (face to face), cofacially ring-stacked polymers, phthalocyanines covalently bound over the ligand to a polymer chain, and many other combinations. Cu—phthalocyanine, as many other phthalocyanines, forms stacked aggregates along the axis perpendicular to the plane of the dye macrocycles. The character of the aggregation is hydrophobic. The substitution of Cu—phthalocyanine with a hydrophilic group like a sulfonic group makes them soluble in aqueous solutions. The equilibrium constants for dimeric aggregation are large and depend on the complexing

metal in the following order $\text{Cu} > \text{H} > \text{Fe} > \text{V} > \text{Zn} > \text{Co} \gg \text{Al}$. Disaggregation of $\text{Cu}(\text{tsPc})^{4-}$ can be achieved with organic solvents (DMSO, pyridine, methanol).

The degree of aggregation plays an important role in the photochemical mechanisms of photooxidation. One of the main features of photodynamic sensitizers is the ability to generate singlet oxygen that is expected to be different for monomers and dimers, because the rate of deactivation by internal conversion to the ground state is suggested to be much greater for dimers.⁸ Contradictory results concerning Cu—phthalocyanine photodynamic activity were reported in the literature. Some reports recorded generation of singlet oxygen,³ the other reports claim that the dyes containing paramagnetic ions (Cu, Fe, V) do not photosensitize the oxidation at all.^{9,10}

Understanding photochemical mechanisms of phthalocyanines plays a crucial role in evaluation of their photodynamic activity and their potential application in PDT therapy. Phthalocyanines have two major absorption bands, namely the B (or Soret) band and the Q band. Photochemical and photophysical behavior of phthalocyanines irradiated with violet or ultraviolet light (resonance with the B band) or visible light in the region 600–700 nm (resonance with the Q band) have been studied very extensively in recent years.^{11–29} It has been found that the commonly accepted pattern of behavior in most photochemical reactions with the rapid deactivation of the higher excited states S_n to the lowest singlet state (S_1) and further dissipation of the energy via fluorescence, intersystem crossing to the lowest excited triplet state (T_1), or internal conversion to the ground state (S_0) may be violated in some groups of compounds including phthalocyanines.²⁹ The higher excited singlet S_n and

triplet T_n states often exhibit fluorescence or phosphorescence, intersystem crossing $S_n \rightarrow T_n$, and enhanced reactivity in electron transfer, energy transfer, or formation of radicals with hydrogen abstraction, competing with rapid deactivation to S_1 state.

There are many fewer papers reporting the photochemical behavior of phthalocyanines induced by irradiation with the vis light that is in resonance neither with the Q band nor the B band because the energies from this range were expected to generate no interesting photochemical features. We will show that the photochemical features revealed in the vis spectral range are very intriguing and shed new light on the photochemistry of phthalocyanines.

In this paper we wish to address the questions about the photochemical and photophysical behavior of $\text{Cu}(\text{tsPc})^{4-}$ induced by laser irradiation with vis light in the range 465–514 nm that is in resonance neither with the Q band (600–700 nm) nor the B band (Soret band) (350 nm). The attempt of the paper is to understand the nature of the emissive states at 527 and 682 nm and the other photochemical and photophysical properties of $\text{Cu}(\text{tsPc})^{4-}$ explored by resonance Raman spectroscopy.

2. Experiment

Spectrograde DMSO and copper(II) phthalocyanine-3,4',4'',4'''-tetrasulfonic acid, tetrasodium salt were purchased from Aldrich. They were used without further purification. Water was distilled before preparing the solutions.

The Raman spectra were recorded in the cryostat (Oxford Instruments Limited) and commercial glass ampules were mounted in a special cell arrangement. The samples were introduced as a liquid, and they were cooled in the cryostat equipped with a heater and thermocouples for temperature monitoring. Cooling the sample was achieved by the use of a 50 L Dewar that supplied a small stream of liquid nitrogen or helium through a vacuum jacketed tube to the cryostat coat. To ensure that the equilibrium phases are generated, the samples were cooled slowly (0.5 °C/min). The nonequilibrium phases were generated at the rapid temperature quenching in a special homemade ring immersed in liquid nitrogen with liquid solutions of $\text{Cu}(\text{tsPc})^{4-}$ injected into the ring. This procedure ensures the maximum possible quenching rate, in contrast to the slow cooling of 0.5 °C/min used for generation of the equilibrium phases. The procedure corresponds to the deposition of an amorphous film or direct sublimation of the sample on the cold support at 77 K used previously to obtain phases strongly deviated from equilibrium.³⁰

Raman spectra were measured with Ramanor U1000 (Jobin Yvon) and Spectra Physics 2017-04S argon ion laser operating at lines 465.8, 472.7, 488, 496.5, and 514 nm at powers 10, 4, 125, 85, and 125 mW, respectively. The Raman spectra in the lattice region 15–200 cm^{-1} and the intramolecular vibrations region 200–7000 cm^{-1} were recorded. The spectra were recorded in a broad temperature range from 293 to 77 K. The spectral slit width was 6 cm^{-1} in the full temperature range, which corresponds to the 500 μm mechanical slit of the spectrometer. A $\lambda/4$ wave plate was used to change the linear polarization into the circular one to avoid the different polarization sensitivity of the gratings. The interference filter has been used to purify the laser line by removing additional natural emission lines that interfere with the Raman lines, especially in the case of solid samples.

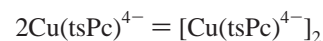
3. Results and Discussion

A. Photochemistry of $\text{Cu}(\text{tsPc})^{4-}$ in Water and DMSO.

Parts a and b of Figure 1 show the Raman spectra of $\text{Cu}(\text{tsPc})^{4-}$

in aqueous solution as a function of temperature for $c = 10^{-2}$ mol/dm^3 and $c = 10^{-3}$ mol/dm^3 , respectively. The similar pattern of behavior has been recorded for other concentrations ranging from $c = 10^{-2}$ to $c = 10^{-5}$ mol/dm^3 . The narrow peaks in the region 200–2000 cm^{-1} correspond to the internal vibrations of $\text{Cu}(\text{tsPc})^{4-}$, the peaks at around 3000 cm^{-1} correspond to the stretching (symmetric and asymmetric) modes of water. In the region 4000–6000 cm^{-1} we can see a very broad, structureless band with the maximum at around 4800 cm^{-1} corresponding to the emission of unknown origin. The emission at the relative wavenumber of 4800 cm^{-1} corresponds to the wavelength of 682 nm for the excitation with the argon laser line 514 nm. The intensity of the emission at 682 nm increases with decreasing temperature. Many phthalocyanines were reported to have fluorescence $S_1 \rightarrow S_0$ for the Q transition in this spectral region.^{29–32} For example, the fluorescence for $\text{Al}(\text{tsPc})$ at 298 K was reported to be 679 nm.³² We have found at 294 K that the excitation with $\lambda = 640$ nm (resonance with the Q transition) leads to the appearance of fluorescence at 682 nm for diluted solutions in DMSO (10^{-6} mol/dm^3) that is completely suppressed for higher concentrations due to the nonradiative deactivation competing effectively with the emissive path. However, the intensity of the fluorescence should decrease, not increase, with the decreasing temperature because the rate of deactivation by internal conversion competes in direct correspondence with the increasing degree of aggregation at low temperatures. It indicates that the emission observed at 682 nm for highly concentrated solutions of $\text{Cu}(\text{tsPc})^{4-}$ in DMSO at low temperatures, although it covers the same spectral range as the Q transition fluorescence at 294 K, should be assigned to the emission of transient species generated by the vis-light irradiation that are stabilized at low temperatures. At room temperature the recombination processes are too fast and the transient species cannot be monitored. We will provide evidence that the emission at 682 nm at low temperatures is not due to the $S_1 \rightarrow S_0$ Q transition fluorescence of $\text{Cu}(\text{tsPc})^{4-}$ and that it originates from the emission of transient radicals generated in photoredox dissociation.

$\text{Cu}(\text{tsPc})^{4-}$ dimerizes readily in aqueous solutions. It tends to aggregate in that solvent even at 10^{-6} mol/dm^3 . Figure 2a shows the absorption spectra of $\text{Cu}(\text{tsPc})^{4-}$ as a function of concentration. One can see that the Q band consists of the bands at 624 and 661 nm corresponding to dimer and monomer, respectively. The dimerization equilibrium constant K for the process



between the monomeric and dimeric forms was calculated from the absorption spectra (Figure 2a) and was found to be 1.15×10^5 in aqueous solution at 294 K. The extinction coefficient is 1.29×10^4 [mol/dm^3] $^{-1}$ cm^{-1} .

To elucidate the differences between the mechanisms of photochemical processes for monomers and dimers of $\text{Cu}(\text{tsPc})^{4-}$, we have studied the photochemistry of $\text{Cu}(\text{tsPc})^{4-}$ in DMSO and compared it with that in aqueous solutions. $\text{Cu}(\text{tsPc})^{4-}$ in DMSO exists almost entirely as monomer, in contrast to water, which is evident from the comparison between the absorption spectra in water and DMSO presented in Figure 2a,b.

Figure 3 shows the Raman spectra of $\text{Cu}(\text{tsPc})^{4-}$ in DMSO solution as a function of temperature for $c = 0.01$ mol/dm^3 . The similar spectra have been recorded for concentrations ranging from $c = 10^{-2}$ to 10^{-5} mol/dm^3 . One can see that like in water, the broad, structureless emission at 682 nm is observed in DMSO at lower temperatures when the solution becomes a

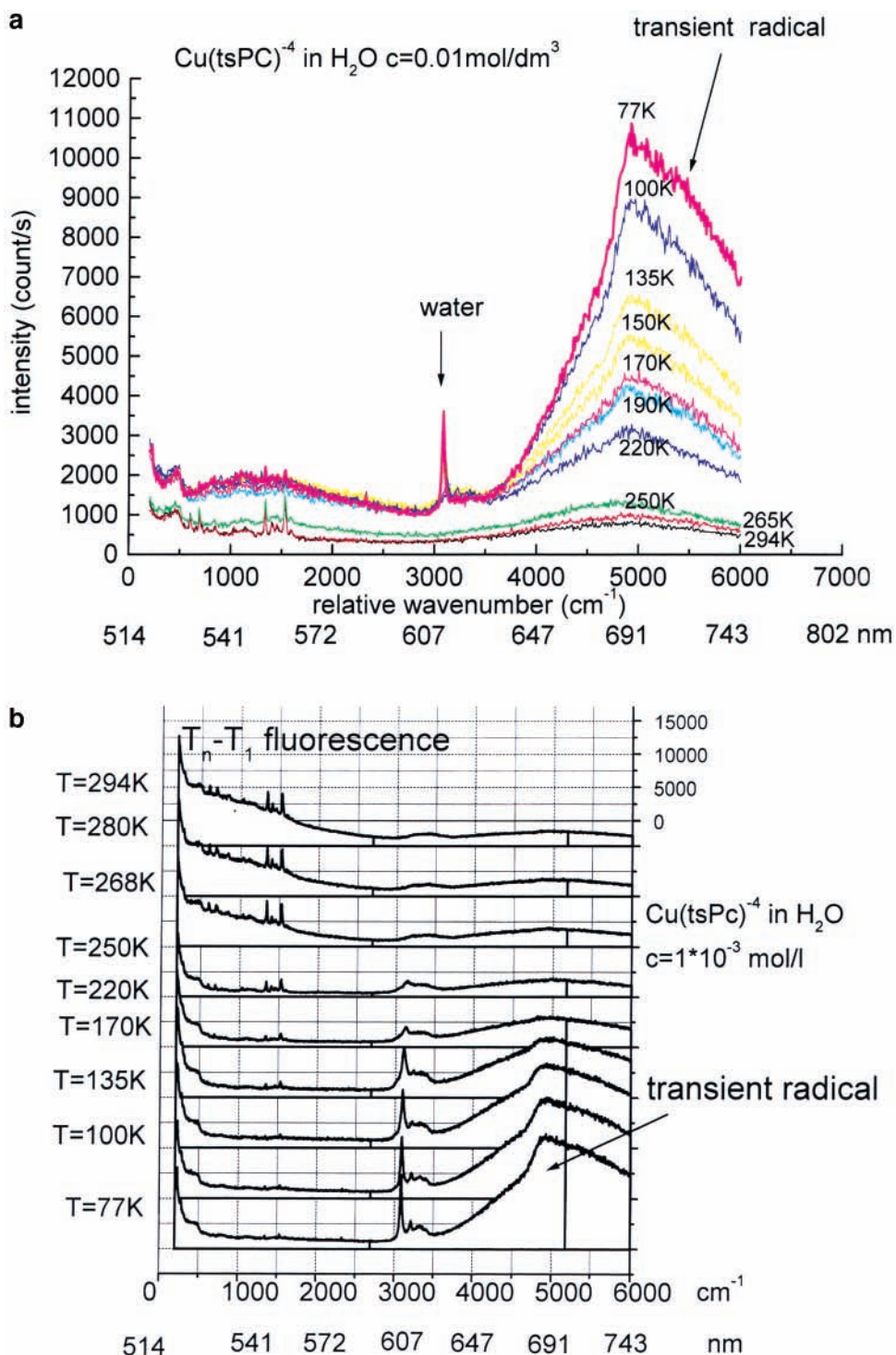


Figure 1. Raman spectra of $\text{Cu}(\text{tsPc})^{4-}$ in aqueous solution as a function of temperature at slow cooling rate (0.5 K/min) for $c = 10^{-2}$ mol/dm³ and $c = 10^{-3}$ mol/dm³.

frozen matrix. The intensity of the band increases with decreasing temperature. However, in contrast to the aqueous solutions (Figure 1a,b) we observe an additional, very intensive emission with the maximum at around 500 cm^{-1} (527 nm). The emission is observed only for liquid solutions and disappears at lower temperatures. At lower temperatures when the solution becomes a frozen matrix, the emission at 527 nm decreases in direct correspondence with the increasing intensity at 682 nm. The isobestic point at around 3400 cm^{-1} (622 nm) indicates that the bands at 527 and 682 nm represent the processes that are linked together. More careful inspection of the spectral features in Figure 3 in the region $4000\text{--}7000\text{ cm}^{-1}$ shows an additional

weak band at 6200 cm^{-1} (754 nm) of unknown origin at 294 K that disappears at lower temperatures.

To understand the origin of the emission at 527 nm in DMSO, we have recorded the Raman spectra as a function of the excitation wavelength. One can see that the intensity of the band at 527 nm depends strongly on the excitation wavelength (Figure 4). The strongest intensity of the emission is observed for the excitation with the wavelength of 465.8 nm. The apparent shift of the emission band maxima in Figure 4 has no physical meaning and simply comes from the fact that the Raman spectra are measured using the relative wavenumbers with respect to the excitation wavenumbers.

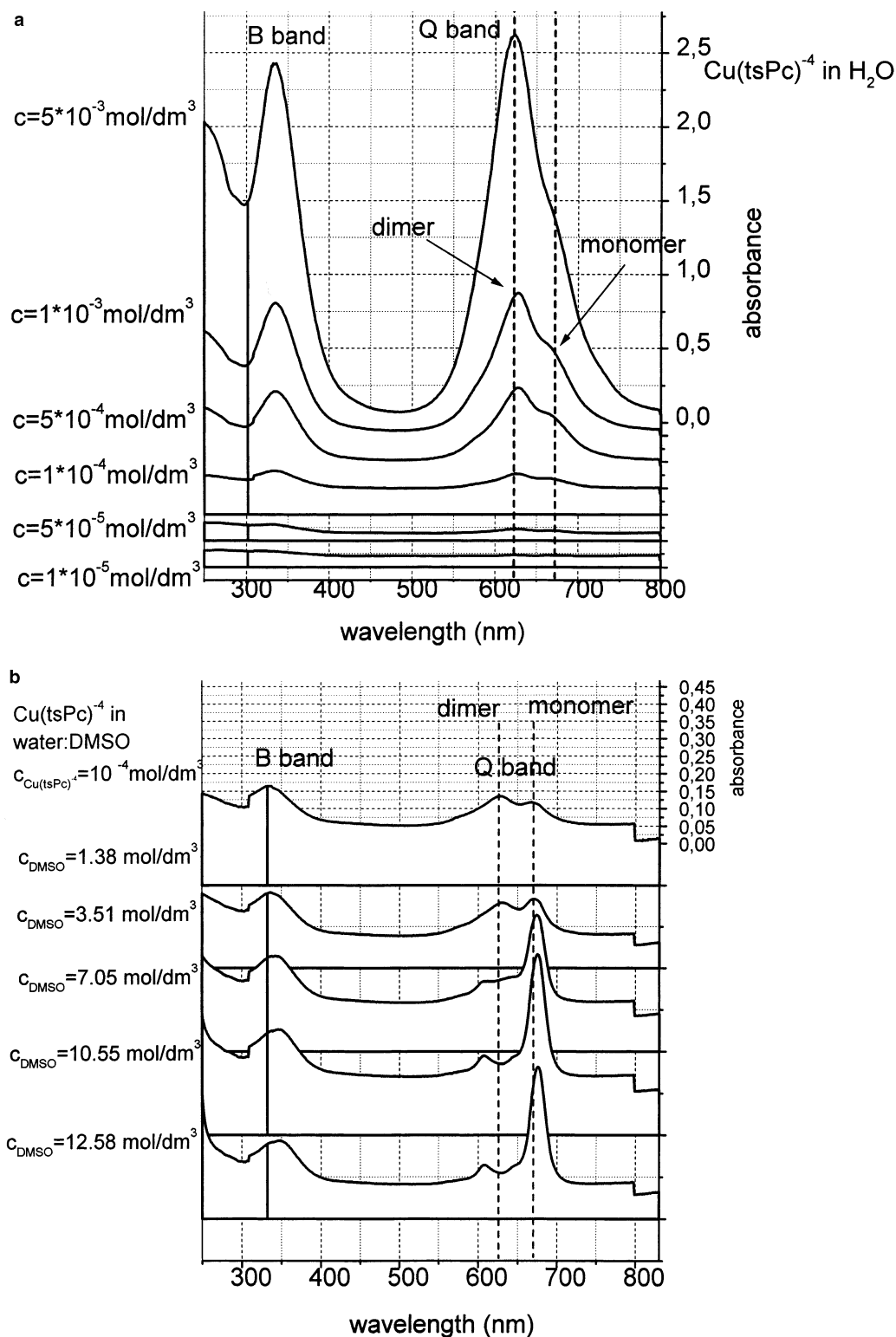


Figure 2. Absorption spectra of $\text{Cu}(\text{tsPc})^{4-}$ at 294 K, optical path = 0.2 mm in aqueous solutions in DMSO.

To decide which of the electronic transitions is in resonance with the irradiation at around 465.8 nm, let us discuss all of the possible electronic transitions in the spectral region under study. One can see from Figure 2a,b that $\text{Cu}(\text{tsPc})^{4-}$ in aqueous and DMSO solutions possesses intense B and Q bands at about 350 nm and between 620 and 670 nm that have been assigned to the transitions between the bonding and antibonding ligand-centered orbitals, ${}^1\pi\pi^*$ ($a_{2u} \rightarrow e_g$ and $a_{1u} \rightarrow e_g$, respectively³²). The existence of four imino nitrogens bridging pyrrole units in the $\text{Cu}(\text{tsPc})^{4-}$ macrocycle (Figure 5) is responsible for the

appearance of the filled nonbonding orbitals and $n\pi^*$ transitions. It has been suggested that the $n\pi^*$ transition is placed ca. 2660 cm^{-1} above the lowest lying ${}^1\pi\pi^*$ ³¹ and it should be observed on the longer wavelength edge of the B band. Because the B and Q bands are strong, these additional transitions that exist between B and Q may mostly be hidden. However, the careful inspection of the absorption measured for a long optical path in this region for $\text{Cu}(\text{tsPc})^{4-}$ in aqueous solution presented in Figure 6 shows evidently weak absorption bands on the longer wavelength edge of the B band at 435 and 460 nm, respectively.

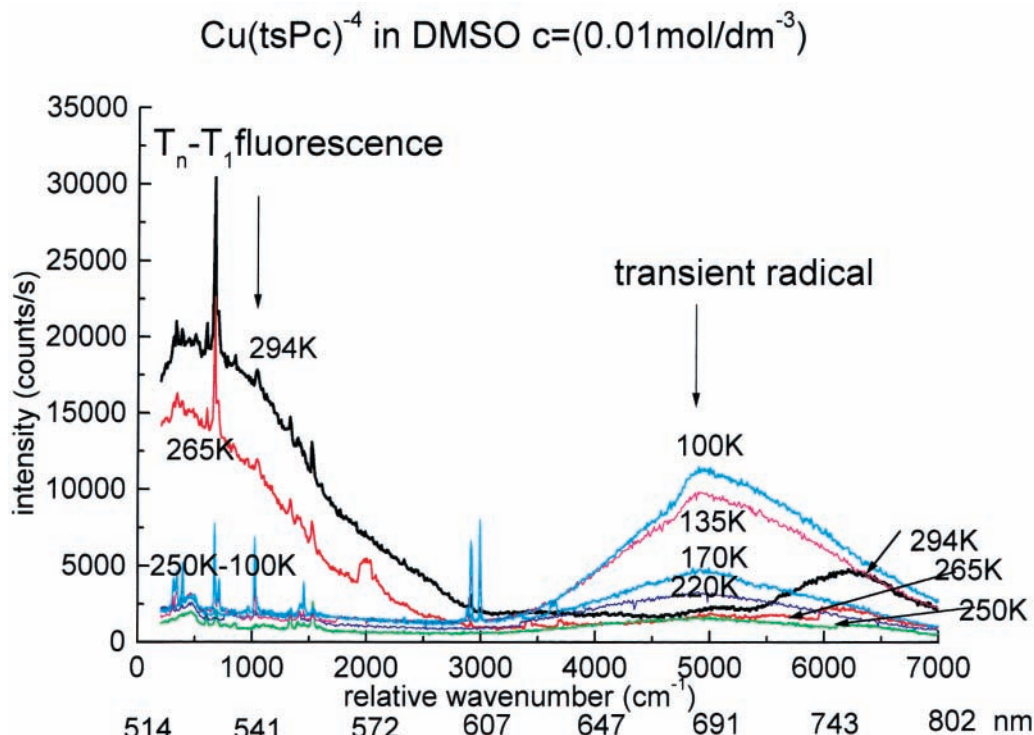


Figure 3. Raman spectra of $\text{Cu}(\text{tsPc})^{4-}$ in DMSO solution as a function of temperature at slow cooling rate (0.5 K/min) for $c = 0.01 \text{ mol/dm}^3$.

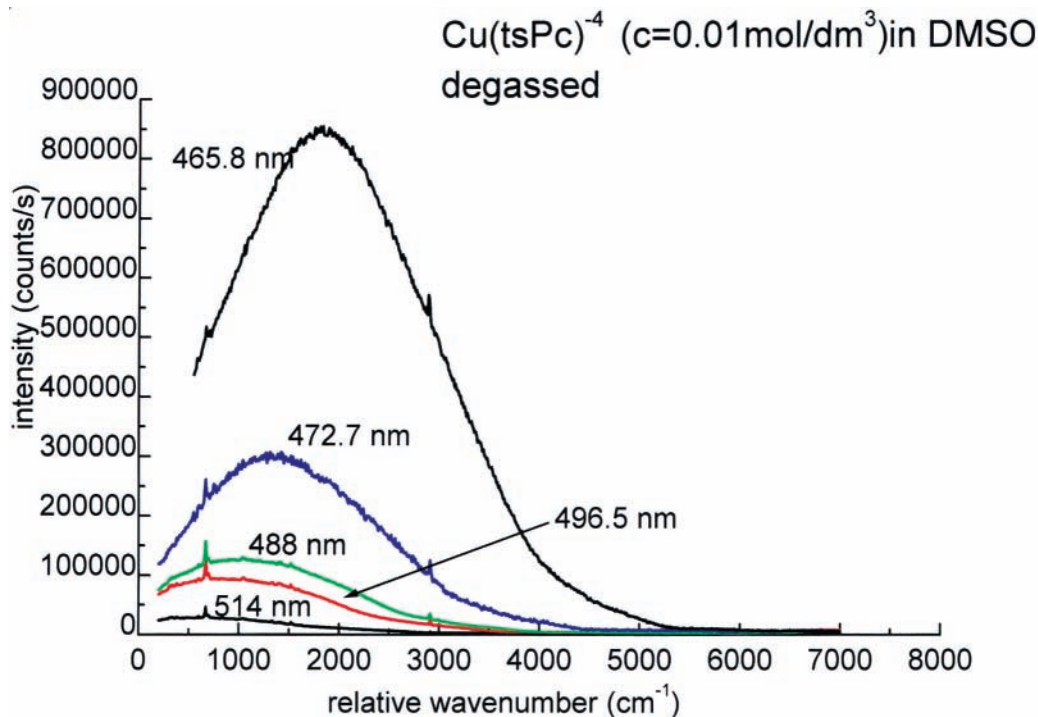


Figure 4. Dependence of the Raman spectra of $\text{Cu}(\text{tsPc})^{4-}$ in DMSO solution (degassed sample) on the wavelength of excitation at 294 K for $c = 0.01 \text{ mol/dm}^3$. The intensities are normalized to the same laser power of 120 mW and the wavelength of 514 nm taking into account the correction of the Raman scattering intensity on the wavelength.

We have assigned the absorption at 435 nm to the $n\pi^*$ transition. The nature of the absorption at 460 nm is less clear. It was reported that the triplet-triplet transition ${}^3\pi\pi^*$ ($T_1 \rightarrow T_n$) is expected in this spectral region.^{9,12} For example, the absorption observed at 480 nm for phthalocyanine (H_2Pc) and copper(II) phthalocyanine (CuPc) has been assigned to the ${}^3\pi\pi^*$ ($T_1 \rightarrow T_n$) transition.⁹ However, the absorption to the higher excited singlet states $S_0 \rightarrow S_n$ has similar energies²⁹ and should be also taken into account for further considerations. The presence of

the emission in the visible region has been reported for many phthalocyanines.¹⁷ In most cases the emission was shown at the longer wavelength side of the B band at around 420–450 nm,^{13,14,17} but in some cases a weak emission was observed at around 500 nm (H_2TsPc , ZnTsPc , Nt-BuPc).^{18,25} The nature of the emissive states in this region is not clear yet. It is obvious that the emission at 527 nm cannot originate from the phosphorescence from the lowest lying excited ligand-centered triplet T_1 state that is shifted to the near-infrared region.³² It

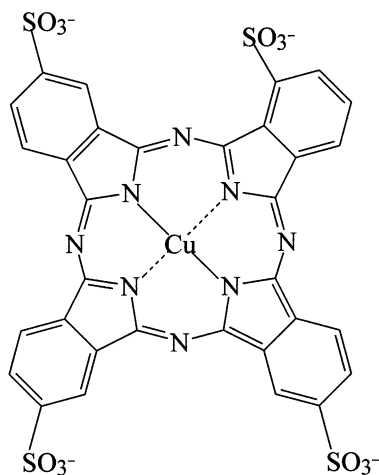


Figure 5. Scheme of $\text{Cu}(\text{tsPc})^{4-}$ macrocycle.

has been suggested that it originates from the higher excited singlet S_n or triplet T_n states of phthalocyanines²⁹ for the Q transition or from the lowest lying excited states of the phthalocyanine radicals.³⁴ If these assignments are correct, the excitation with 465.8 nm in Figure 4 leads to the resonance with the electronic transition ${}^3\pi\pi^*$ ($T_1 \rightarrow T_n$) or ${}^1\pi\pi^*$ ($S_0 \rightarrow S_n$) and populates the higher excited triplet T_n or singlet S_n states that may be followed by the fluorescence at 527 nm. The emission at 527 nm is also observed in the preresonance conditions for irradiation with 514 nm in DMSO (Figure 3) whereas it is not observed in aqueous solutions (Figure 1a).

To provide a more convincing argument supporting the assignment of the emissive band at 527 nm to the fluorescence from the higher excited triplet state ($T_n \rightarrow T_1$), we have performed various energy transfer experiments and particularly the experiments with sensitization of oxygen triplets. In Figure 7 we have compared the intensity of the band for $\text{Cu}(\text{tsPc})^{4-}$ in aqueous solution in degassed and nondeareated sample. One can see that the intensity of the emission at 1500 cm^{-1} (556 nm) is significantly suppressed in nondeareated aqueous solu-

tions when compared with degassed samples, confirming singlet oxygen involvement in the process of deactivation of the triplet state T_n .

The assignment of the fluorescence at 556 nm (in water) and 527 nm (in DMSO) to the $T_n \rightarrow T_1$ transition raises a question about the mechanism of populating the lowest lying triplet state T_1 . It seems that the vis light from the range 465.8–514 nm with an energy in excess for the Q transition (${}^1\pi\pi^*$, $a_{1u}(\pi) \rightarrow e_g(\pi^*)$) populates the vibrationally excited states that are deactivated rapidly to the ground vibrational state of the lowest lying excited singlet state S_1 ($e_g(\pi^*)$). The resulting S_1 state undergoes intersystem crossing to the lowest excited triplet state T_1 . This mechanism seems to be supported by the clear vibrational structure of the Q electronic transition in DMSO with peaks at 610 and 675 nm (Figure 2b). The frequency of the vibrational mode that is coupled the most efficiently to the electronic transition estimated from the vibrational structure has been found to be 1522 cm^{-1} and closely corresponds to the ν_4 vibrational mode at 1527 cm^{-1} monitored by the resonance enhanced Raman signal (Figure 8).

B. Electron Transfer. In view of the results presented so far we can state that the vis photochemistry of $\text{Cu}(\text{tsPc})^{4-}$ monomers (in DMSO) and dimers (in H_2O) differs significantly. The emissive band at 527 nm in Figure 3 is observed in both nondeareated and degassed samples of $\text{Cu}(\text{tsPc})^{4-}$ in DMSO at 294 K without any changes in the intensity as function of time, whereas it disappears immediately after the irradiation in nondeareated samples and much slower in degassed samples in H_2O at 556 nm (Figure 7). The stationary Raman technique applied in the paper does not allow us to estimate exactly the time scale of the decay, but this finding clearly indicates that singlet oxygen quenching is not the only mechanism responsible for the deactivation of the excited triplet state T_n . There must exist an additional mechanism (or mechanisms) of deactivation of the T_n state (or the S_1 and T_1 states) that is competitive to the $T_n \rightarrow T_1$ fluorescence.

To consider possible mechanisms of deactivation, it is helpful to recall that the mechanisms of quenching are very sensitive

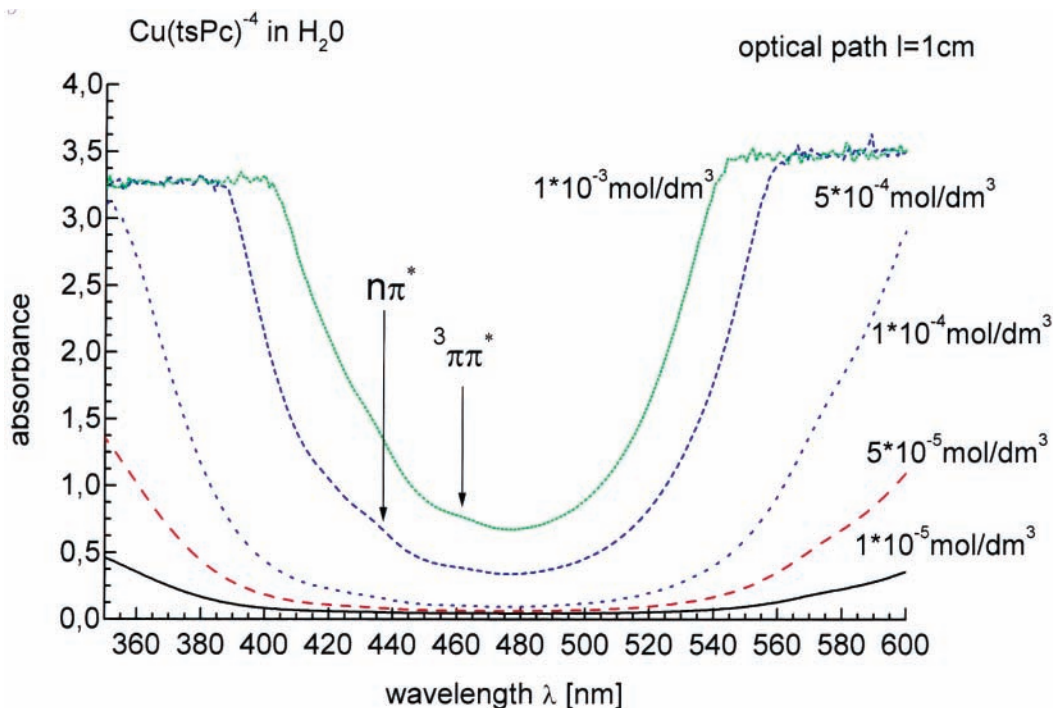


Figure 6. Absorption spectra of $\text{Cu}(\text{tsPc})^{4-}$ in aqueous solutions at 294 K, optical path = 1 cm.

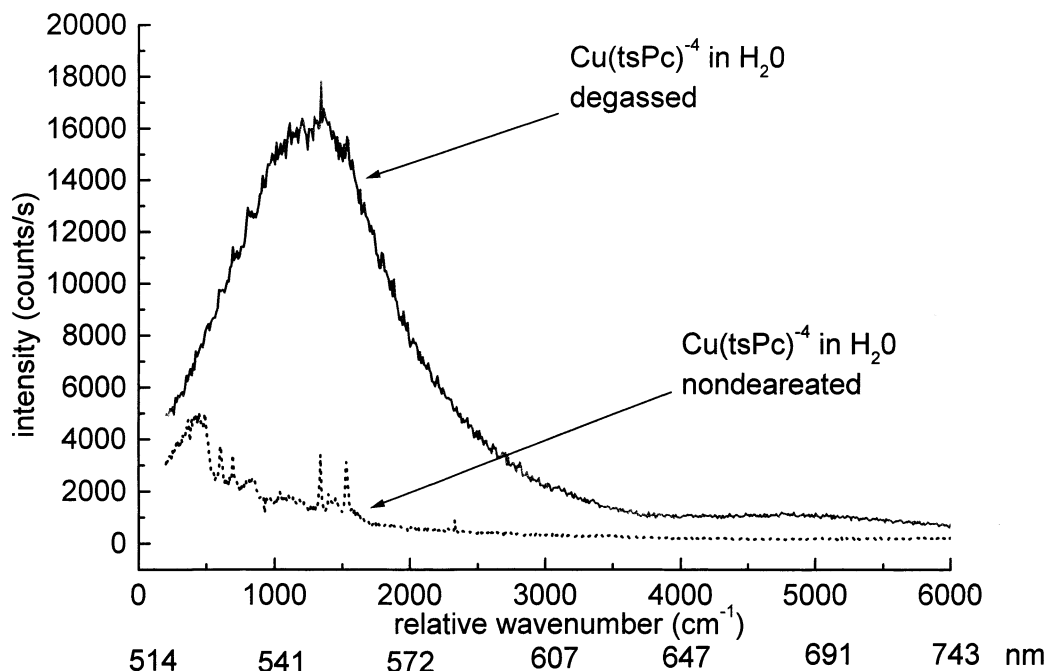


Figure 7. Raman spectra of $\text{Cu}(\text{tsPc})^{4-}$ in aqueous solution for nondegassed and degassed samples at 294 K for $c = 10^{-2} \text{ mol/dm}^3$.

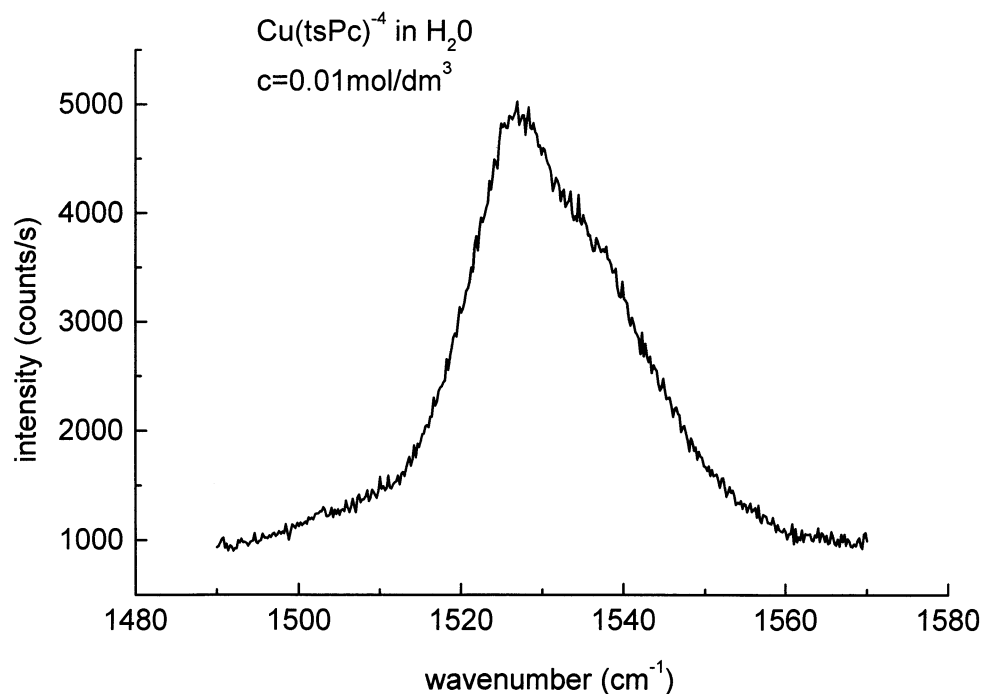
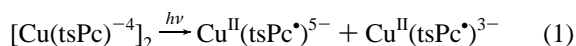


Figure 8. Raman band shape of the ν_4 vibrational mode of $\text{Cu}(\text{tsPc})^{4-}$ macrocycle in DMSO solution (degassed sample) at 294 K.

to the degree of aggregation. It was reported³² that the irradiation of phthalocyanines with the wavelengths corresponding to the resonance with the B transition or with the shorter wavelengths induces the photoredox dissociation:



The photoredox dissociation (eq 1) leads to the electron transfer between the adjacent molecules that results in formation of the ligand radical species $\text{Cu}^{\text{II}}(\text{tsPc}^{\bullet})^{5-}$ and $\text{Cu}^{\text{II}}(\text{tsPc}^{\bullet})^{3-}$. Our results presented so far strongly suggest that there must exist an additional mechanism (or mechanisms) of deactivation of the T_n state (or the T_1 state) that is competitive to the $T_n \rightarrow T_1$ fluorescence. It seems to be very likely that these additional

mechanisms of deactivation are related to the formation of the transient radicals. To verify this possibility, we have to check if the energies from the visible region used for irradiation of the sample are sufficient to generate the transient radical species. Because the redox energies for the monomers and the enthalpy of dimerization for $\text{Cu}(\text{tsPc})^{4-}$ are known from literature,³² it is possible to compare the energy required to induce the photoredox dissociation (1) with the energy of the irradiation used in this paper. Figure 9 shows the semiquantitative energy diagram of the excited states of $\text{Cu}(\text{tsPc})^{4-}$ in aqueous solutions and the relative energies of reduction and oxidation of the macrocycle E ($\text{Pc}/\text{Pc}^{\bullet-}$) and E ($\text{Pc}^{\bullet+}/\text{Pc}$) in the monomeric $\text{Cu}(\text{tsPc})^{4-}$. We can state from Figure 9 that the excitation energies applied in this paper (463.8–514 nm) are sufficient to

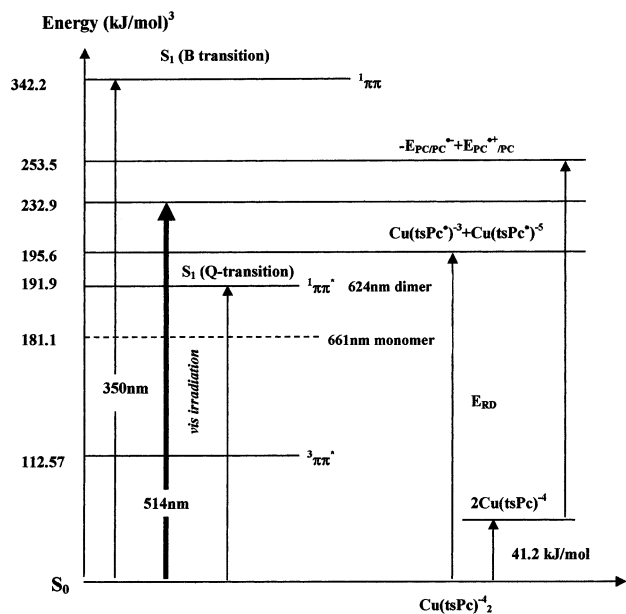


Figure 9. Semiquantitative energy diagram of excited states in $\text{Cu}(\text{tsPc})^{4-}$ in aqueous solutions relating to the relative energies of reduction and oxidation of the macrocycle in the monomeric $\text{Cu}(\text{tsPc})^{4-}$. E_{RD} is the threshold energy for the photoredox dissociation; $E(\text{Pc}^+/\text{Pc}^{\bullet-})$ and $E(\text{Pc}^{\bullet+}/\text{Pc})$ are the standard reduction and oxidation energies of the macrocycle in the monomeric phthalocyanine.³²

induce the redox photodissociation (1) resulting in formation of $\text{Cu}^{\text{II}}(\text{tsPc}^{\bullet})^{5-}$ and $\text{Cu}^{\text{II}}(\text{tsPc}^{\bullet})^{3-}$ radicals. It indicates that the vis light may generate transient radicals that live very shortly at room temperatures and compete in the deactivation of the T_n state. With decreasing temperature the recombination reaction rates become slower and the emission from the transient radicals can be observed. In view of the results presented so far it becomes clear that the emission at 682 nm must be related to the presence of $\text{Cu}^{\text{II}}(\text{tsPc}^{\bullet})^{5-}$ and $\text{Cu}^{\text{II}}(\text{tsPc}^{\bullet})^{3-}$ radicals generated in the photoredox dissociation (1).

C. Origin of the 682 nm Emission: Photochemistry of $\text{Cu}(\text{tsPc})^{4-}$ in Crystals and Glasses. To establish firmly the

assignment, let us discuss in detail the nature of the emission at 682 nm observed for $\text{Cu}(\text{tsPc})^{4-}$ in both water (Figure 1a,b) and DMSO (Figure 3). Although the emission at 682 nm occurs in the same spectral range as the fluorescence $S_1 \rightarrow S_0$ for the Q electronic transition for $\text{Cu}(\text{tsPc})^{4-}$ in very diluted DMSO solutions (10^{-6} mol/dm³) at 294 K we will provide further evidence that the low-temperature emission at 682 nm represents the transient radicals that are generated in the photoredox dissociation (1) induced by irradiation with vis light.

To provide a more convincing argument in supporting the assignment of the band 682 nm to the phthalocyanine radicals, we have performed the low-temperature Raman measurements at various rates of cooling. It is well-known that distinct structures of matrixes are generated at rapid and slow cooling rates.³³ Rapid cooling usually generates the glassy frozen matrixes, whereas a slow cooling rate leads to the crystal matrixes. The generated phases can be easily monitored by the low-frequency Raman spectra where phonon peaks signal the existence of translationally ordered crystal structure whereas the absence of any phonon peaks indicates that the glassy phase has been formed. The results we presented so far in Figures 1a,b and 3 are related to the slow cooling rate that generates the crystal structures of $\text{Cu}(\text{tsPc})^{4-}$ in both H₂O and in DMSO. It would be interesting to compare the results for the crystal phase with those in the glassy phase.

Figure 10 shows the Raman spectrum of $\text{Cu}(\text{tsPc})^{4-}$ in DMSO ($c = 10^{-2}$ mol/dm³) for the rapid cooling when the glassy structure has been generated at 77 K. A similar spectrum has been recorded for $\text{Cu}(\text{tsPc})^{4-}$ in an aqueous glassy matrix. Striking behavior is revealed when Figure 3 (for the crystal structure) is compared with Figure 10 (for the glassy structure). First, there is no band at 4800 cm⁻¹ (682 nm) for the glassy phase in contrast to that observed in the crystal phases at 77 K. Second, the band at 527 nm that exists only for the liquid solutions at higher temperatures and disappears at low temperatures for the crystal phase (Figure 3) still exists in the glassy phase at 77 K (Figure 10). It looks like the photochemical properties of the liquid state have been preserved in the amorphous glassy phase. It clearly indicates that the structure

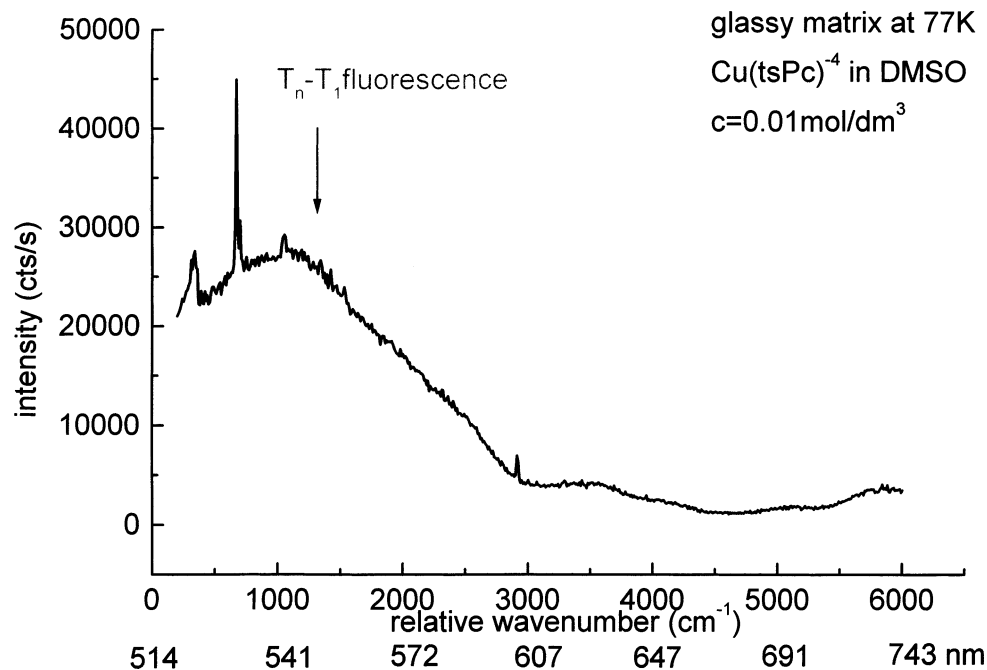


Figure 10. Raman spectrum of $\text{Cu}(\text{tsPc})^{4-}$ in DMSO for $c = 10^{-2}$ mol/dm³ for the rapid cooling when the glassy structure has been generated at 77 K.

of $\text{Cu}(\text{tsPc})^{4-}$ has a profound influence on the photochemical behavior. The crystal polymorphs of $\text{Cu}(\text{tsPc})^{4-}$ form ring-stacked columns³⁴ close enough in space to overlap efficiently between the π -electronic clouds, and as a consequence, the photoinduced electron transfer between the adjacent macromolecule rings occurs, leading to the photoinduced dissociation (eq 1).

In contrast to the crystal phases, the liquid solutions and amorphous glassy phases are only partially organized. As a consequence, the distances between the adjacent phthalocyanine rings are longer and the overlapping between π -electronic clouds is much less efficient, resulting in much less efficient photoinduced electron transfer (1).

The above statements can rationalize the different pattern of photochemistry for the slow and rapid cooling as well as the photochemistry in different solvents. Indeed, the irradiation with vis wavelengths excites the higher triplet state T_n , which is deactivated to the T_1 state exhibiting emission at 527 nm (DMSO) and 556 nm (H_2O) or competitively deactivated via radiationless quenching by the photoreduction process (1). The radiationless photoreduction quenching is a much more efficient path for deactivation of the T_n state in aqueous solution (dimers) at ambient temperatures and in crystal matrixes (both in water and DMSO) at low temperatures than for DMSO solutions (monomers) and glassy matrixes (both in water and DMSO) as a consequence of much less efficient overlapping between π -electron clouds. This is the reason the band at 527 nm is observed in Figures 3 and 10 whereas it disappears in Figure 1a,b. In contrast, the band at 682 nm (4800 cm^{-1}) is not observed for the glassy phase in Figure 10 whereas it has a very strong intensity for the crystal phases in Figures 1a,b and 3. The disappearance of the band at 527 nm is accompanied by the appearance of the band at 682 nm that clearly indicates the emission at 682 nm must be related to the photoredox dissociation and the ligand radical species.

To specify whether the emission at 682 nm is related to $\text{Cu}^{\text{II}}(\text{tsPc}^{\bullet})^{5-}$ or $\text{Cu}^{\text{II}}(\text{tsPc}^{\bullet})^{3-}$ radicals, we have performed a series of measurements in the presence of radical cation and radical anion scavengers. We have found that the intensity of the band at 682 nm is suppressed by the presence of radical cation scavengers such as triethylamine. Thus, we have assigned the emission at 682 nm to the $\text{Cu}(\text{tsPc}^{\bullet})^{3-}$ radical. This assignment corresponds very well with another experimental finding that the $\text{Cu}^{\text{II}}(\text{tsPc}^{\bullet})^{3-}$ radical has an absorption at $\lambda = 515\text{ nm}$.^{32,35,36} So, it becomes clear that the vis irradiation at $\lambda = 514\text{ nm}$ excites the phthalocyanine radicals to the excited electronic state $\text{Cu}(\text{tsPc}^{\bullet})^{3-} \xrightarrow{h\nu} {}^*\text{Cu}(\text{tsPc}^{\bullet})^{3-}$ that emits fluorescence as the system approaches the ground state.

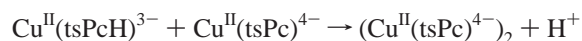
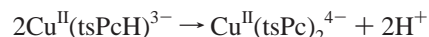
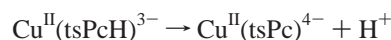
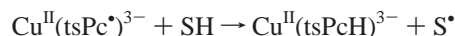
D. Photochemistry of $\text{Cu}(\text{tsPc})^{4-}$ in Water–Alcohol Mixtures. The question arises why we have not assigned the emission at 527 nm to the $\text{Cu}^{\text{II}}(\text{tsPc}^{\bullet})^{3-}$ radical. Feraudi et al.³⁶ assigned the transient absorption at around 500 nm to the radical cation $\text{Cu}^{\text{II}}(\text{tsPc}^{\bullet})^{3-}$. So, it would be appealing to assign the emission at 527 nm to the emission of the phthalocyanine radicals instead of to the $T_n \rightarrow T_1$ fluorescence of phthalocyanine $\text{Cu}(\text{tsPc})^{4-}$, as we propose in this paper.

To discuss this issue, it is worth remembering that the excited states of the radicals are competitively quenched by (a) recombination of dimeric species through intramolecular electron transfer, which regenerates phthalocyanine $\text{Cu}(\text{tsPc})^{4-}$, and (b) decomposition processes. In the presence of the radical scavengers, copper phthalocyanine radicals may form a transient product associated with the abstraction of hydrogen (in protic solvents) $[\text{Cu}^{\text{II}}(\text{tsPcH})^{3-}]$ or an adduct or peroxo compound

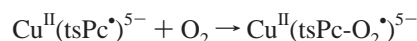
$[\text{Cu}^{\text{II}}(\text{tsPc}-\text{O}_2)^{5-}]$. All these competitive processes become less effective with decreasing temperature because the molecular motions become slower. This is one of the main reasons we have not assigned the emission at 527 nm to the copper phthalocyanine radicals. The emission at 527 nm cannot represent the fluorescence from the radicals because this assumption would lead to unreasonable conclusions that the photoredox dissociation (1) takes place more effectively during irradiation of phthalocyanine monomers (in DMSO, Figure 3) than dimers (in water, Figure 1a,b) and that the regeneration of the dimer $\text{Cu}^{\text{II}}(\text{tsPc}^{\bullet})^{5-} + \text{Cu}^{\text{II}}(\text{tsPc}^{\bullet})^{3-} = [\text{Cu}(\text{tsPc})^{4-}]_2$ occurs faster at low temperatures.

To provide further evidence that the emission at 527 nm cannot result from the phthalocyanine radicals we have performed the resonance Raman measurements for $\text{Cu}(\text{tsPc})^{4-}$ in water–alcohol (methanol, 1-propanol) mixtures. The results for water–methanol are presented in Figure 11. One can see that the intensity of the band at 527 nm decreases in direct correspondence with the increasing intensity of the band at 682 nm when temperature decreases. The isobestic point can be clearly seen at 4000 cm^{-1} (647 nm). This point corresponds exactly to the wavelength of the crossover between the band of the dimer (624 nm) and monomer (661 nm) in Figure 2a,b.

Let us examine the other possible transients that may be generated in protic solvents and in the presence of oxygen. The interception of the oxidized species $\text{Cu}^{\text{II}}(\text{tsPc}^{\bullet})^{3-}$ with alcohols leads to the stabilization of the reduced species $\text{Cu}^{\text{II}}(\text{tsPc}^{\bullet})^{5-}$ and generation of a transient product associated with the abstraction of hydrogen in the following sequence of reactions



With decreasing temperature the sequence of reactions between the oxidized species of phthalocyanine and the protic solvent SH that leads to the recombination of phthalocyanine dimers becomes slower. If we assumed that the emission at 527 nm comes from the protonated isomer of the monomeric phthalocyanine $[\text{Cu}^{\text{II}}(\text{tsPcH})^{3-}]$, it would imply that the intensity of the emission at 527 nm should increase, not decrease, with decreasing temperature, in contrast to the experimental results in Figure 11. On the other hand, if we assume that the emission at 527 nm comes from the excited state of the reduced species $\text{Cu}^{\text{II}}(\text{tsPc}^{\bullet})^{5-}$, we should take into account that the interception of the reduced species with oxygen does not prevent the recombination of the dimer. Because Figure 11 presents the results for the sample that was not degassed the following sequence of reactions may occur



Again, the rate of the reactions leading to the recombination of the dimers $(\text{Cu}^{\text{II}}(\text{tsPc})^{4-})_2$ should be slower for lower temperatures, which would imply that the emission of the band 527 nm should increase with decreasing temperature, in contrast to the experimental results in Figure 11.

One can see from Figure 11 that the intensity of the band 527 nm decreases whereas the intensity of the band 682 nm

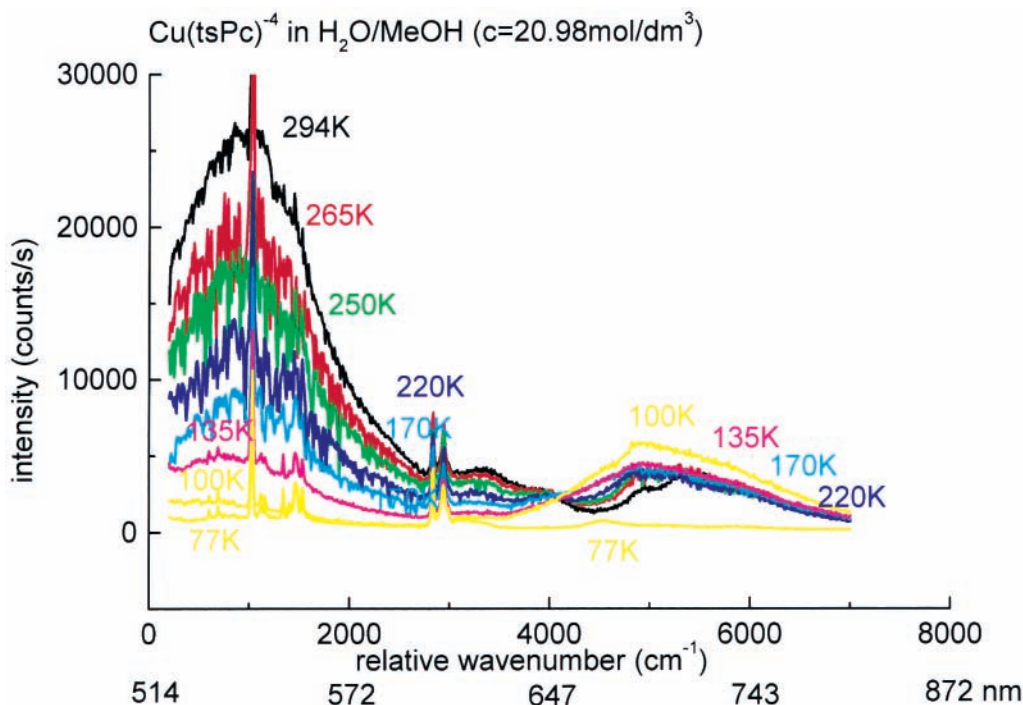


Figure 11. Raman spectra of $\text{Cu}(\text{tsPc})^{4-}$ in water-methanol mixtures as a function of temperature at slow cooling rate (0.5 K/min) for $C_{\text{Cu}(\text{tsPc})^{4-}} = 0.001 \text{ mol/dm}^3$, methanol concentration $c = 20 \text{ mol/dm}^3$.

increases with decreasing temperature. Similar results were obtained in Figure 3 in DMSO solution, which, in contrast to methanol, is an aprotic solvent. It indicates that the band 527 nm does not represent the protonated species $[\text{Cu}^{\text{II}}(\text{tsPcH})^{3-}]$. In contrast to aqueous solutions, the dimerization constant of $(\text{Cu}^{\text{II}}(\text{tsPc})^{4-})$ in methanol like in DMSO is totally displaced toward the monomeric species, preventing the electron transfer in the photoredox dissociation (1). Thus, the results strongly suggest that the different photochemistry in aqueous solutions in comparison with DMSO and alcohols is associated with the monomer–dimer equilibrium than with the acid–base equilibrium.

The picture that emerges from the analysis to this point shows clearly that the photochemical behavior of $\text{Cu}(\text{tsPc})^{4-}$ is entirely determined by the photoredox dissociation. It is not still quite clear if the photoinduced redox dissociation occurs in the lowest lying singlet S_1 state or in the higher triplet state T_n . The knowledge of the reduction potentials for the excited singlet and triplet states would be very helpful because the reduction potentials may differ significantly for the triplet and singlet states,³² resulting in different reactivity. Unfortunately, the reduction potentials for $\text{Cu}(\text{tsPc})^{4-}$ in the higher triplet states are unknown.

Let us look at the schematic diagram of the energy levels in Figure 9 and the photochemical sequence of events after the vis irradiation that we propose in this paper (Figure 12). One can see from Figure 9 that the energy of the pair $\text{Cu}^{\text{II}}(\text{tsPc}^{\bullet})^{5-} + \text{Cu}^{\text{II}}(\text{tsPc}^{\bullet})^{3-}$ is comparable with the energy of the vibrationally excited singlet state S_1 for the Q transition. Fast relaxation of the vibrational states is in competition with the photoredox dissociation that may occur directly from the S_1 state or by the population of the lowest lying triplet state T_1 followed by the excitation to the T_n state. The temperature dependence of the $T_n \rightarrow T_1$ fluorescence cannot provide a hint which state (S_1 or T_n) is involved in the photoredox dissociation because the intensity of the $T_n \rightarrow T_1$ fluorescence would decrease with decreasing temperature in both cases. However, applying the energies from Figures 9 and 12, one can estimate the energy

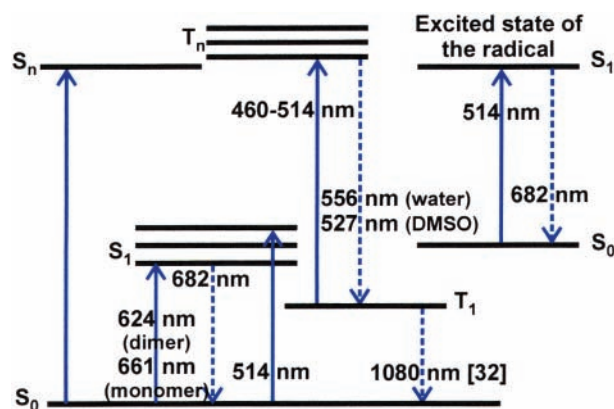


Figure 12. Schematic energy diagram of excited states of $\text{Cu}(\text{tsPc})^{4-}$ for the Q transition.

difference between the ground state of the radical and the triplet state T_n . We have found that it corresponds to the wavelength of 678 nm and is in perfect agreement with the experimentally observed emission at 682 nm. This provides strong evidence that the photoredox dissociation occurs in the T_n state.

4. Conclusions

The vis light irradiation of the copper(II) phthalocyanine-3,4',4'',4'''-tetrasulfonate anion $\text{Cu}(\text{tsPc})^{4-}$ with the energy between the B transition (350 nm) and the Q transition (600–700 nm) leads to the mechanisms of photophysical and photochemical behavior presented in Figure 12.

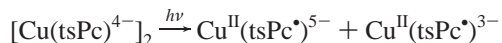
1. vis light excites the ground-state S_0 of the molecule to the vibrationally excited states of the lowest lying singlet excited state (S_1) for the Q transition



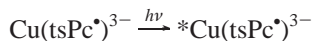
where v is the vibrational quantum number. The vibrational mode coupled to the electronic Q transition estimated from the

vibronic structure of the Q band in DMSO was found to be ν_4 (1530 cm^{-1}).

2. No fluorescence ($S_1 \rightarrow S_0$) is observed when the sample is irradiated with $\lambda = 514\text{--}465\text{ nm}$ in contrast to the irradiation with $\lambda = 640\text{ nm}$ (resonance with Q transition) for which the fluorescence at 682 nm is recorded for very dilute (10^{-6} mol/dm^3) DMSO liquid solutions. It indicates that the radiative channel of deactivation via fluorescence is in strong competition with the intersystem crossing (ISC) to the excited triplet state (T_1) and the photoredox dissociation when irradiated with the energies sufficient to generate transient radicals. The vis light irradiation with $\lambda = 514\text{--}465\text{ nm}$ of $\text{Cu}(\text{tsPc})^{4-}$ dimers leads to the photoredox dissociation immediately upon excitation and generation of the transient radicals



The vis irradiation with $\lambda = 514\text{--}465\text{ nm}$ excites the molecules from the excited triplet state T_1 to the higher excited triplet state T_n that emits the fluorescence at 527 nm for $\text{Cu}(\text{tsPc})^{4-}$ in DMSO and at 556 nm in H_2O . The emission in aqueous solutions is significantly suppressed in nondeareated samples. In addition, the vis irradiation excites the phthalocyanine radicals that are generated in the photoredox dissociation to the lowest lying excited electronic state



The excited state of the radical emits fluorescence at 682 nm followed by the return to the ground state of the radical. The intensity of the radical emission increases with decreasing temperature as the competitive processes of deactivation become less effective due to slower molecular motions.

3. At higher temperatures in liquid solutions the fate of the radicals is determined by (a) recombination of dimeric species according to eq 1, (b) associative disproportionation and decomposition processes, and (c) radiationless deactivation of the excited states of the radicals through hydrogen abstraction ($\text{Cu}^{\text{II}}(\text{tsPcH})^{3-}$) or forming a peroxo compound ($\text{Cu}^{\text{II}}(\text{tsPc-O}_2)^{5-}$).

We have shown that the photoinduced dissociation with the electron transfer between the molecules of $\text{Cu}(\text{tsPc})^{4-}$ is determined by the distance between the adjacent rings and the structure. The electron transfer that leads to the generation of the ligand-centered radicals may occur only for the ring-stacked structures with strong overlapping between the π -electronic clouds. These structures exist only in highly concentrated aqueous solutions and in the crystal phases. The photoinduced electron transfer does not occur for the monomers of $\text{Cu}(\text{tsPc})^{4-}$ in liquid DMSO solution and in the glassy phases.

The photochemistry of metallophthalocyanines is a very exciting and promising subject for further investigation. The attempt to elucidate the dynamics of the photochemical processes by femtosecond time-resolved spectroscopy has been made in our laboratory, and progress in this area is very promising. The results will be published in subsequent papers.

Acknowledgment. We gratefully acknowledge the support of this work by KBN through grant 1236T09/2001/20. The support from the Dz.S/03 is also acknowledged.

References and Notes

- Rosenthal, I.; Ben-Hur, E. In *Phthalocyanines. Properties and Applications*; Leznoff, C. C., Lever, A. B., Eds.; VCH Publishers: New York, 1989; p 393.
- Bonnett, R.; Martinez, G. *Tetrahedron* **2001**, *57*, 9513.
- Wu, S. K.; Zhang, H. C.; Cui, G. Z.; Xu, D. N.; Xu, H. J. *Acta Chim. Sinica* **1985**, *43*, 10.
- Bonnett, R. *Rev. Contemp. Pharmacother.* **1999**, *10*, 1.
- Monahan, A. R.; Brado, J. A.; DeLuca, A. F. *J. Phys. Chem.* **1972**, *76*, 1994.
- Abkowitz, M.; Monahan, A. R. *J. Chem. Phys.* **1973**, *58*, 2281.
- Wohrle, D. In *Phthalocyanines. Properties and Applications*; Leznoff, C. C., Lever, A. B., Eds.; VCH Publishers: New York, 1989; p 55.
- Darwent, J. R.; Douglas, P.; Harriman, A.; Porter, G.; Richoux, M. C. *Coord. Chem. Rev.* **1982**, *44*, 83.
- McVie, J.; Sinclair, R. S.; Truscott, T. G. *J. Chem. Soc. Faraday Trans. 2* **1978**, *74*, 1870.
- Tokumaru, K.; Kaneko, Y. In *Phthalocyanines*; Shirai, H., Kobayashi, N., Eds.; IPC: Tokyo, 1997; p 224.
- Tokumaru, K. In *Phthalocyanines*; Shirai, H., Kobayashi, N., Eds.; IPC: Tokyo, 1997; p 170.
- Prasad, D. R.; Ferraudi, G. *Inorg. Chem.* **1982**, *21*, 2967.
- Muralidharan, S.; Ferraudi, G. *J. Phys. Chem.* **1983**, *87*, 4877.
- Ferraudi, G.; Muralidharan, S. *Inorg. Chem.* **1983**, *22*, 1369.
- Kaneko, Y.; Arai, T.; Sakarugi, H.; Tokumaru, K.; Pac, C. J. *Photochem. Photobiol. A: Chem.* **1996**, *97*, 155.
- Kaneko, Y.; Nishimura, Y.; Arai, T.; Sakarugi, H.; Tokumaru, K.; Matsunaga, D. *J. Photochem. Photobiol. A: Chem.* **1995**, *89*, 37.
- Kaneko, Y.; Nishimura, Y.; Takane, N.; Arai, T.; Sakarugi, H.; Tokumaru, K.; Kobayashi, N.; Matsunaga, D. *J. Photochem. Photobiol. A: Chem.* **1997**, *106*, 177.
- Howe, I.; Zhang, J. Z. *J. Phys. Chem. A* **1997**, *101*, 3207.
- Ruckmann, I.; Zeug, A.; Herter, R.; Roder, B. *Photochem. Photobiol.* **1997**, *66*, 576.
- Chahraoui, D.; Valet, P.; Kossanyi, J. *Res. Chem. Intermed.* **1992**, *17*, 219.
- Kobayashi, N.; Ashida, T.; Osa, T. *Chem. Lett.* **1992**, 2031.
- Kobayashi, N.; Lever, A. B. P. *J. Am. Chem. Soc.* **1987**, *109*, 7433.
- Kobayashi, N.; Lam, H.; Nevin, W. A.; Leznoff, C. C.; Koyama, T.; Monden, A.; Shirai, H. *J. Am. Chem. Soc.* **1994**, *116*, 879.
- Kobayashi, N.; Togashi, M.; Osa, T.; Ishii, K.; Yamauchi, S.; Hino, H. *J. Am. Chem. Soc.* **1996**, *118*, 1073.
- Zhong, Q.; Wang, Z.; Liu, Y.; Zhu, Q.; Kong, F. *J. Chem. Phys.* **1996**, *105*, 5377.
- Strickler, S. J.; Berg, R. A. *J. Chem. Phys.* **1962**, *37*, 814.
- Gilbert, A.; Baggott, J. *Essentials of molecular Photochemistry*; Blackwell: Oxford, U.K., 1991; p 98.
- Rosenthal, I.; Krishna, C. M.; Riesz, P.; Ben-Hur, E. *Radiat. Res.* **1989**, *107*, 136.
- Tokumaru, K. *J. Porphyrins Phthalocyanines* **2001**, *5*, 77.
- Johari, G. P.; Hallbrucker, A.; Mayer, E. *J. Chem. Phys.* **1990**, *92*, 6743.
- Schaffer, A. M.; Gouterman, M.; Davidson, E. R. *Theor. Chim. Acta* **1973**, *30*, 9.
- Ferraudi, G. In *Phthalocyanines. Properties and Applications*; Leznoff, C. C., Lever, A. B., Eds.; VCH Publishers: New York, 1989; p 321.
- Angell, C. A. *Science* **1995**, *267*, 1924.
- Simon, J.; Bassoul, P. In *Phthalocyanines. Properties and Applications*; Leznoff, C. C., Lever, A. B., Eds.; VCH Publishers: New York, 1989; p 223.
- Geiger, D. K.; Ferraudi, G.; Madden, K.; Granifo, J.; Rillema, D. P. *J. Phys. Chem.* **1985**, *89*, 3890.
- Ferraudi, G.; Srisankar, E. V. *Inorg. Chem.* **1978**, *17*, 3164.